Numerical Modeling of Torpedo Anchors

by

M. Raie, Graduate Research Assistant
and
J. L. Tassoulas, Principal Investigator
The University of Texas at Austin

Final Project Report – Phase I
Prepared for the Minerals Management Service
Under the MMS/OTRC Cooperative Research Agreement
1435-01-04-CA-35515
Task Order 39344
MMS Project Number 557

September 2006

OTRC Library Number: 9/06B174

"The views and conclusions contained in this document are those of the authors and should not be interpreted as representing the opinions or policies of the U.S. Government. Mention of trade names or commercial products does not constitute their endorsement by the U. S. Government".

For more information contact:

Offshore Technology Research Center
Texas A&M University
1200 Mariner Drive
College Station, Texas 77845-3400
(979) 845-6000

or

Offshore Technology Research Center
The University of Texas at Austin
1 University Station C3700
Austin, Texas 78712-0318
(512) 471-6989

A National Science Foundation Graduated Engineering Research Center

Table of Contents

List of Tables and Figures

Numerical Modeling of Torpedo Anchors
Phase I Report

M. Raie, Graduate Research Assistant
and
J.L. Tassoulas, Principal Investigator

Offshore Technology Research Center

Abstract

This report summarizes our progress to date in the development of a computational procedure to predict the embedment depth of torpedo anchors. The procedure uses a computational fluid dynamics (CFD) model to evaluate resisting forces on the anchor. The CFD model is applied to vertical penetration of axisymmetric soil penetrators. Apart from promising results regarding the embedment depth as well as the velocity profile, the procedure provides estimates of the pressure and shear distributions on the soil-anchor interface. These distributions will be used in computations of soil reconsolidation in the vicinity of the anchor for the purpose of set-up studies, in preparation for pull-out capacity estimation.

Introduction

Recent oil explorations in the Gulf of Mexico have indicated major reserves beyond the continental shelf, in water depths of 1,500 m to 3,000 m. In order to produce oil from such depths, an economically and technically practical anchoring system should be used for floating units. In 1977, the concept of free-fall, deadweight anchor was proposed as a cost-effective and feasible option for ocean thermal energy conservation power plants (Atturio and Valent, 1977). Petrobras started development of a torpedo-shaped, free-fall anchor in 1996 as a device for mooring flexible risers and floating structures. A torpedo anchor is installed by its kinetic energy, acquired during free fall of 30 to 150 m through the water before penetrating the seabed. It is a cylindrical steel pipe with a conical tip and a padeye at the top, filled with scrap steel and concrete to increase the weight and maintain the center of gravity below the center of buoyancy (Medeiros et al., 1997; Ayabe et al., 2001). Medeiros (2002) reported the first commercial application of torpedo anchors in January 2000 for anchoring flexible risers in the Campos Basin, offshore Brazil. Petrobras used more than ninety finless torpedo anchors, 0.76 m in diameter, 12 m in length and 240 kN in weight from January 2000 to December 2001 for anchoring flexible risers. Torpedo anchors with the same diameter and length but weighing 421 kN with four longitudinal fins were used for anchoring mobile offshore drilling units. Longitudinal fins were attached along the half-upper part of the anchor to increase its directional stability during free fall. In order to anchor a floating production storage and offloading (FPSO) unit in water depth of 1400 m with required holding capacity of 7500 kN, a torpedo anchor 1.07 m in diameter, 17 m in length and 961 kN in weight was designed (Araujo et al.,2004). Lieng et al. (1999, 2000) proposed a similar concept, referred to as deep penetrating anchor (DPA), for anchoring offshore. This anchor is 1.2 m in diameter, 13 m in length, weighs 740 kN and has a blunt massive tip and four thick fins attached to its upper part, while the shank is filled with concrete containing a percentage of steel. The center of gravity is above the center of buoyancy but calculations show that viscous drag forces on the fins prevent rotation of the anchor during free fall. Zimmerman and Spikula (2005) suggested an improved design of a torpedo anchor. This new design is called self-penetrating embedment attachment rotating (SPEAR) anchor. The SPEAR anchor is arrow-shaped and the padeye is at the middle of the anchor length. It is claimed that the holding capacity and reliability of the SPEAR anchor exceed those of the torpedo anchor and deep penetrating anchor.

Ehlers et al. (2004) have suggested that the following anchors are suitable for taut-leg mooring of deepwater floating systems where the anchor has to withstand significant pull-out forces: suction caisson anchor, vertically loaded anchor, suction embedded plate anchor and torpedo anchor. The torpedo anchor has three advantages over other alternatives. First, it is economical because an external source of energy is not required for installation. It is also economical because of easy fabrication, quick installation with a single anchor-handling vessel and limited use of remotely-operated vehicles. In addition, more anchors per trip can be transported to the site because of the compact size of torpedo anchors compared to suction caissons. Second, the installation is less sensitive to environmental conditions. Finally, the anchor holding capacity is less sensitive to the initial estimate of soil shear-strength profile. It is rather a function of input energy

(O'Loughlin et al., 2004). The disadvantage of the torpedo anchor is uncertainty in verticality of the anchor, which affects the holding capacity (Ehlers et al., 2004)

Brandao et al., 2006 reported laboratory model tests with different configurations of ballast inside the anchor in order to reduce anchor inclination during installation. They concluded that lead can be used as pile ballast to lower the center of gravity and consequently reduce the inclination. They also reported installation of eighteen torpedo anchors weighing 961 kN for mooring FPSO P-50 in the Albacora Leste field. Three of these anchors were recovered and deployed again due to excessive inclination of more than 10 degrees. The measured inclination of one anchor during installation was found to be between 15 to 30 degrees but after initial penetration the inclination is reduced to its final value of 8.3 degrees. All other anchors showed a similar behavior.

A series of studies were coordinated by the Nuclear Energy Agency to evaluate the feasibility of high-level radioactive waste disposal through free-fall, cylindrical projectiles in oceanic sediments. Freeman et al. (1984) carried out instrumented model penetrator tests toward design of a stable projectile in water, achieving maximum possible penetration into the seabed. A streamlined projectile measuring 3.25 m in length, 0.325 m in diameter and weighing 1.8 tonnes, the European Standard Penetrator (ESP), reached impact velocity of about 50 m/s. The disturbance caused by shear due to rather unlikely current of 1 m/s produces a small, 1°, inclination with respect to the vertical direction at velocity of 50 m/s. Damping of this disturbance appears to be greater than critical and its amplitude decays rapidly. It was also reported that misalignment of fins produces deviation of the penetrator from the vertical path. Hickerson et al. (1988) found that stability, besides ocean currents and fin misalignment, is a principal factor affecting the penetrator trajectory inside the water. The stability depends primarily on the distance between the gravity center and the hydrodynamic center. This distance can be controlled by adding ballast and adjusting the arrangement and size of the fins. In a desirable design, the gravity center should be lower than the hydrodynamic center by 10 % of the anchor length.

Installation Analysis

The purpose of installation analysis is the estimation of the embedment depth of the torpedo anchor. Clearly, the final embedment depth of torpedo anchor plays an important role in subsequent behavior of the anchor because its holding capacity is directly related to the strength of the soil that typically increases with depth. Furthermore, installation analysis leads to estimation of forces resisting penetration and, possibly, improved design of the torpedo anchor, achieving deeper penetration and, consequently, higher holding capacity.

Analytical Method

True (1975, 1976) developed an analytical method to predict the undrained vertical penetration of cylindrical penetrators into ocean-bottom sediments. The differential equation governing the anchor motion can be written as:

$$M^* \cdot \frac{dv}{dt} = W' - S_e \cdot (F_{BE} + F_{AD}) - F_H \qquad (1)$$

where M^* = effective mass of penetrator: the mass of penetrator plus the added mass of the surrounding soil

W' = submerged weight of penetrator in soil

F_{BE} = bearing pressure force (end bearing force)

F_{AD} = side adhesion force (shaft friction force)

F_H = inertial drag force

S_e = soil strain-rate effect

True assumed that the added mass is constant during penetration, equal to twice the volume of the anchor times the density of soil, and derived an averaged strain-rate effect from penetration data as a function of penetrator instantaneous velocity. The bearing pressure and side adhesion forces are provided by the conventional static ultimate pile capacity estimates, with few adjustments, as expressed in following equations:

$$F_{BE} = S_u \cdot N_c \cdot A_F \qquad (2)$$

$$F_{AD} = S_u \cdot \delta \cdot \frac{A_S}{S_t} \qquad (3)$$

where S_u = static undrained soil shear strength

N_c = bearing capacity factor

A_F = penetrator frontal area

δ = side adhesion factor

A_S = penetrator side area

S_t = soil sensitivity, ratio of undisturbed to remolded static shear strength

The undisturbed shear strength in the side-adhesion term is divided by the soil sensitivity on account of the remolding condition around the shaft. True assumed that the side adhesion force is reduced by the outward momentum of the soil produced around the nose of advancing penetrator which tends to separates the soil from the shaft. The following expression (based on experimental data) was suggested for high penetration velocities:

$$\delta = 1 - \exp\left(\frac{1}{8} - \frac{L}{40 \cdot D \cdot \tan(\alpha)}\right) \text{ , for } \frac{L}{D \cdot \tan(\alpha)} \geq 5 \qquad (4a)$$

$$\delta = 0 \text{ , for } \frac{L}{D \cdot \tan(\alpha)} < 5 \qquad (4b)$$

where L = penetrator length

D = penetrator diameter

α = penetrator nose half-angle

The drag formula in fluids was utilized to evaluate the inertial drag force of the soil as:

$$F_H = \frac{1}{2} \cdot \rho \cdot C_D \cdot A_F \cdot v^2 \qquad (5)$$

where ρ = soil mass density

C_D = fluid drag coefficient based on frontal area

A_F = penetrator frontal area

v = penetrator velocity

True recommended using an averaged drag coefficient equal to 0.7 for a variety of penetrator geometries and velocities in his tests. Finally, a finite-difference method was used in solving the above differential equation (Eq. 1).

Beard (1984), Freeman and Burdett (1986), O'Loughlin et al. (2004) and Audibert et al. (2006) employed a similar prediction method for the embedment depth and concentrated their efforts on refining the estimates of soil resisting forces. It is important to keep in mind that accurate estimation of anchor effective mass, inertial drag force and side-adhesion factor at high velocities of penetration is not straightforward. Also, it is rather unclear how details of penetrator geometry, e.g. nose shape, can be taken into account in True's approach. Finally, while the differential equation (Eq. 1) will provide the velocity profile during penetration (and the final embedment depth), True's procedure will not produce information regarding the deformation of the surrounding soil or the distribution of pressure and shear along the penetrator.

CFD Modeling

Toward overcoming the limitations of the analytical model described above, a procedure based on computational fluid dynamics (CFD) modeling was developed and applied to predict the embedment depth of soil-penetrating anchors and the pressure and shear distributions along the anchors. The CFD model is capable of simulating the installation of the torpedo anchor from the release point to the final embedment depth, including the transition of anchor from water into the soil. It is worth noting that the parameters of the CFD model were derived in terms of fundamental properties of the soil.

FLUENT models and solvers

FLUENT is a CFD computer program based on the finite-volume method, capable of modeling moving objects in a multiphase domain. The Segregated solver handles the governing equations of continuity and momentum sequentially while the Six-Degree-of-Freedom solver keeps track of rigid-body falling of the anchor. The Volume-of-Fluid model was chosen for the analysis of multiple immiscible phases. The layering method was used in updating the mesh in each time step. High soil viscosity gives a low Reynolds number. Thus, a laminar-flow model was specified. The soil is modeled using a non-Newtonian Bingham fluid with shear-thinning (pseudo-plastic). In non-Newtonian fluids, the viscosity is a function of the strain-rate. One type of non-Newtonian fluid is the Bingham plastic, distinguished by a non-zero shear stress at zero strain-rate. The Bingham plastic model is used to produce the equivalent of plastic forces (end bearing and shaft friction forces) on the penetrator. The shear-thinning model is required to

simulate the strain-rate effect in the soil correctly. Shear-thinning behavior is available through a Power-Law viscosity model. Bingham and Power-Law behaviors are combined in the Herschel-Bulkley model (FLUENT User's Guide, 2006), defined by the following equations:

$$\tau = \tau_0 + \kappa(\dot{\gamma}^n - \dot{\gamma}_0{}^n) \text{ , for } \dot{\gamma} > \dot{\gamma}_0 \qquad (6a)$$

$$\tau = \mu_0 \cdot \dot{\gamma} \qquad \text{, for } \dot{\gamma} \le \dot{\gamma}_0 \qquad (6b)$$

where τ = shear stress

τ_0 = yield shear stress

κ = consistency index

$\dot{\gamma}$ = strain rate

$\dot{\gamma}_0$ = yield strain rate

n = power-law index

μ_0 = yielding viscosity

A subroutine based on the Herschel-Bulkley model was added to the program to model the soil. The strain-rate effect of soil was taken into account by specifying the consistency index and the power-law index in the Herschel-Bulkley model. Specifically, the yield stress was set equal to the soil shear strength through the depth. The effect of remolded soil around the shaft was included in the model by dividing the soil shear strength by the soil sensitivity while the bearing pressure force at the tip was simulated by providing an equivalent shear stress on the basis of increased yield shear stress at the tip. Setting the right-hand side of Eq. 2 for end bearing force equal to the integral of yield shear stress over the tip surface, the required yield shear stress in the tip region is given by:

$$\tau_{0,tip} = \frac{1}{\pi} \cdot \frac{A_F}{A_T} \cdot N_c \cdot S_u \qquad (7)$$

where $\tau_{0,tip}$ = required yield shear stress at the tip

S_u = static undrained soil shear strength

N_c = bearing capacity factor

A_F = penetrator frontal area

A_T = projected area of the tip on a plane parallel to the penetrator longitudinal axis

Results

The model tests reported by True (1976) for axisymmetric penetrators in soft silts were used to verify the CFD computational procedure. Two tests were chosen with a pointed penetrator. In these tests, a launching gun was used to shoot the penetrator into the soil. The impact velocity was measured equal to 6.54 m/s for the first test and equal to 8.23 m/s for the second test. Figure 1 shows the geometry of the moving body, consisting of the penetrator (lower part), accelerometer housing (middle part) and launching shaft (top

part). The mass of the moving body is equal to 0.342 kg, the penetrator length is equal to 0.143 m and the penetrator nose angle is 28°. The gravity center of the moving body is located at about one third of the total length of the moving body from the conical tip. In the computations, the penetrator is assumed rigid. A picture (True, 1976) of the penetrator suggests that its surface of penetrator was polished. However, no comment on this matter was made in the report (True, 1976).

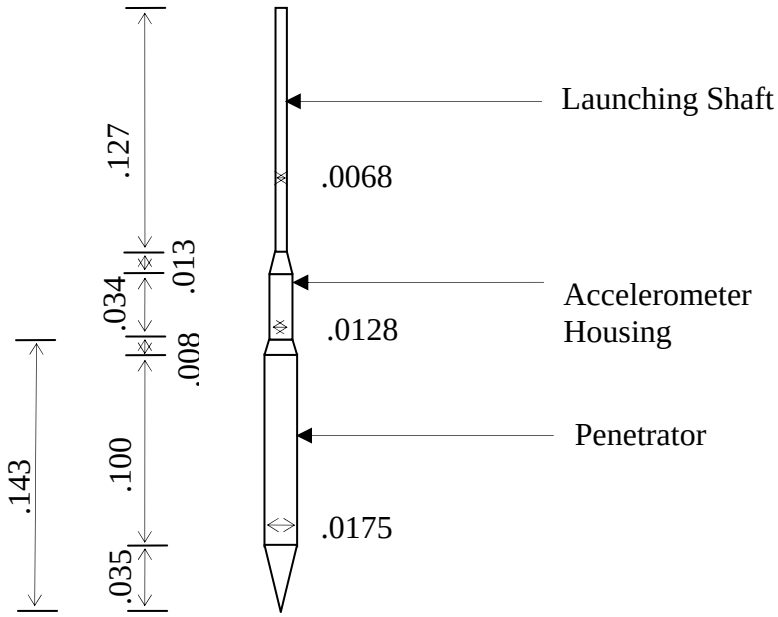

Figure 1: Geometry of moving body (dimensions are in meters)

Both tests were carried out in a tank with constant soil shear strength through the depth, equal to 1,765 Pa, and soil sensitivity equal to 1.5. The soil properties, penetrator characteristics, impact velocities and (measured) embedment depths are summarized in Tables 1 and 2.

Table 1: Soil properties

Parameter	Description	Saturated density	Sensitivity	Shear strength
Units	-	kg/m3	-	Pa
Test 1	soft silt	1400	1.5	1765
Test 2	soft silt	1400	1.5	1765

Table 2: Penetrator characteristics, impact velocities and embedment depths

Parameter	Mass*	Diameter	Length	Nose angle	Material	Impact velocity	Embedment depth
Units	kg	m	m	Deg.	-	m/s	m
Test 1	0.342	0.0175	0.143	28	steel	6.54	0.299
Test 2	0.342	0.0175	0.143	28	steel	8.23	0.413

*includes the mass of the penetrator, accelerometer housing and launching shaft

A mesh-size sensitivity analysis was carried out to determine the appropriate mesh size for the analysis. Figure 2 shows that a fine mesh is used around the penetrator, gradually coarsening away from the penetrator. Figure 3 indicates the soil volume fraction at an instance during the penetration process. It shows that the soil is not in contact with the upper embedded part of the shaft, verifying the use of the reduced side-adhesion factor in True's method (Eqs. 4a and 4b). Figures 4 and 5 display the pressure and shear distributions along the penetrator, respectively, corresponding to the location of anchor in Figure 3 for the first test. In Figure 4, the minimum pressure is related to the point where the soil separates from the shaft. It can be seen from Figure 5 that the tip shear is higher than the shaft shear due to increased yield shear stress at the tip (see Eq. 7). The shear on the upper embedded part of the shaft (where a gap is present between the shaft and the soil) is almost zero. Similar pressure and shear distributions for the second test are indicated in Figures 6 and 7. A 10 % increase in shear strength per tenfold increase in strain rate is required to calibrate the final embedment depth in the first test. This is equivalent to specifying the consistency index equal to 2800 and power-law index equal to 0.321 in the Herschel-Bulkley model. Subsequently, the calibrated model was used to predict the embedment depth of the second test. The CFD-procedure prediction for the second test is practically identical to the measurement. True has already calibrated his procedure with his experiments. However, in the present study, the soil strain-rate effect in True's Method (S_e) was calibrated using the first test. The calibrated True's Method gives a small, 2 %, error in predicting the embedment depth in the second test. While the differences between True's method and the CFD procedure are very small, it is worth noting that the CFD procedure remains closer than True's method to the velocity profile throughout the penetration process (see Figures 8 and 9).

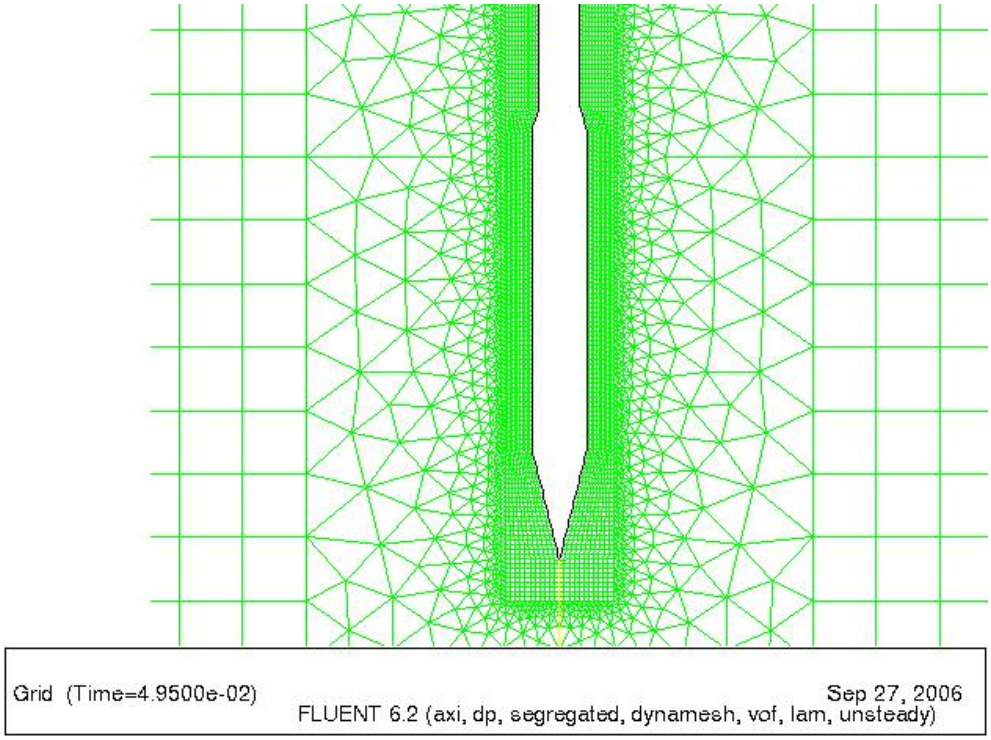

Figure 2: Mesh around the penetrator

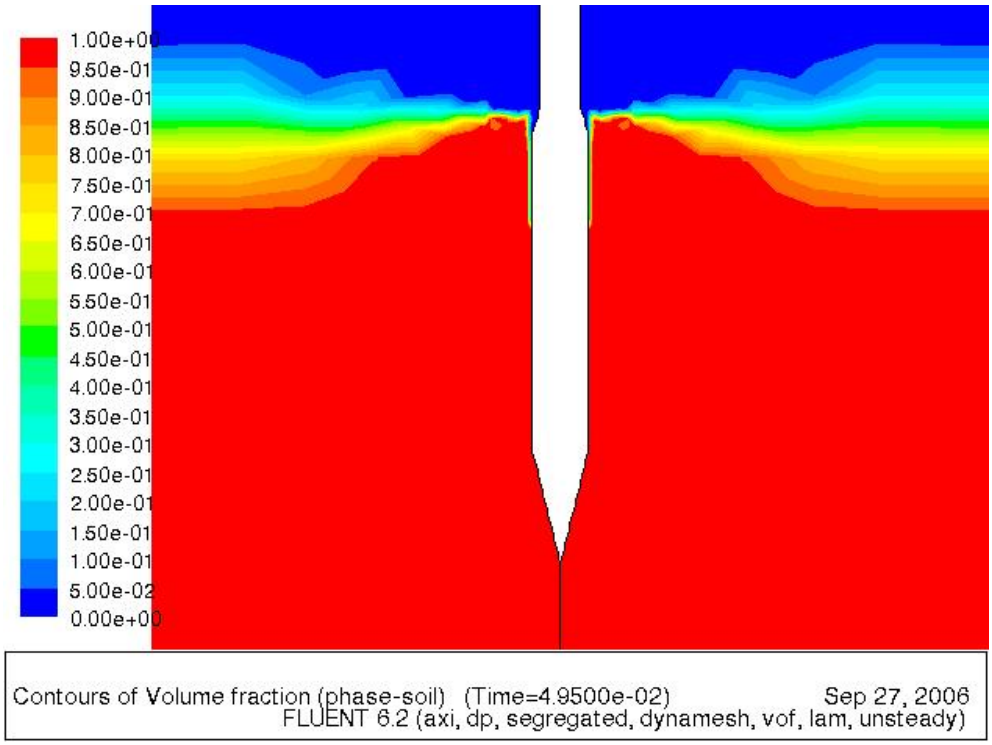

Figure 3: Volume fraction of soil at an instance during penetration

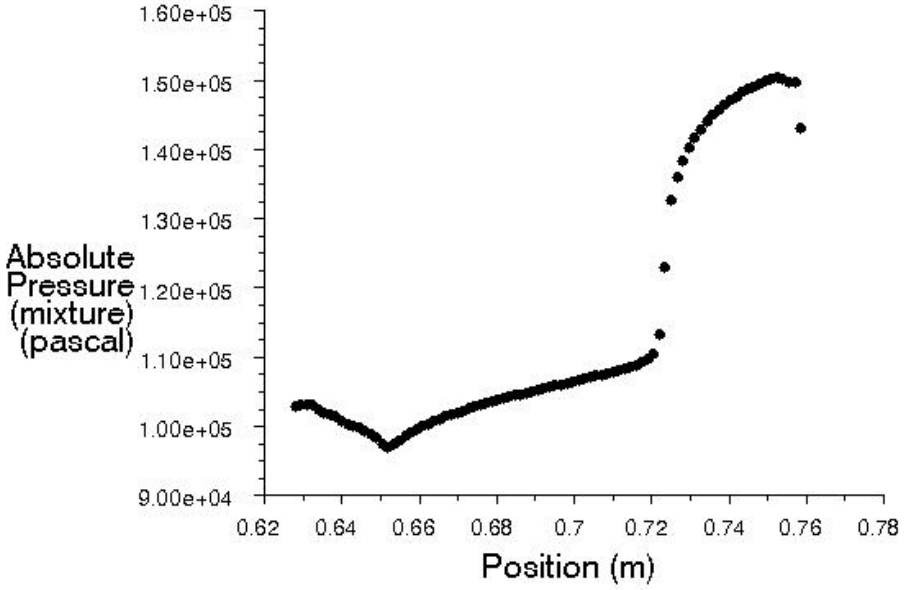

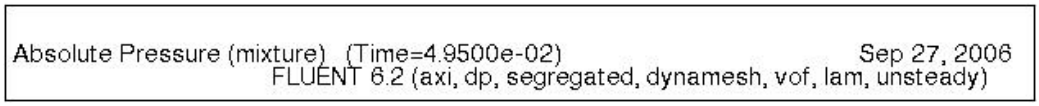

Figure 4: Pressure distribution along the penetrator for the first test

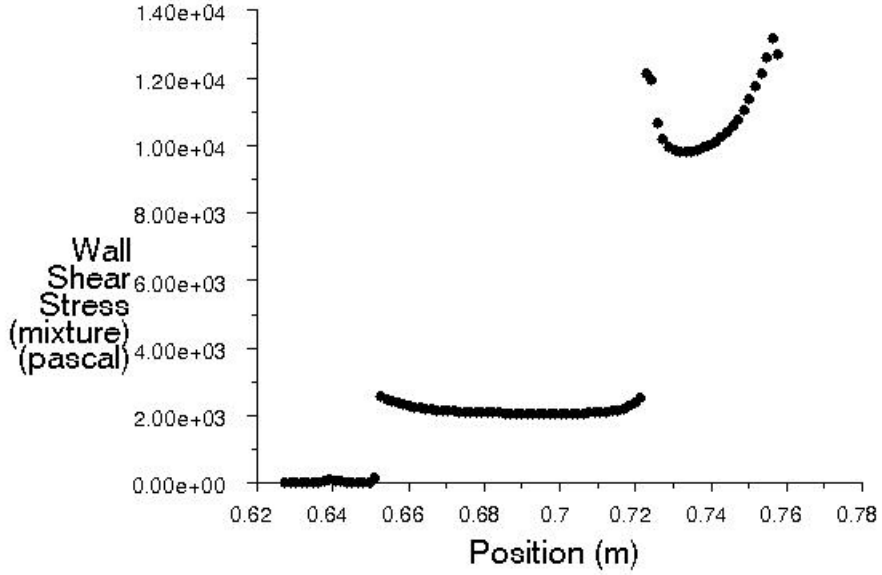

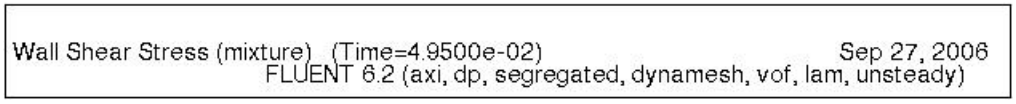

Figure 5: Shear distribution along the penetrator for the first test

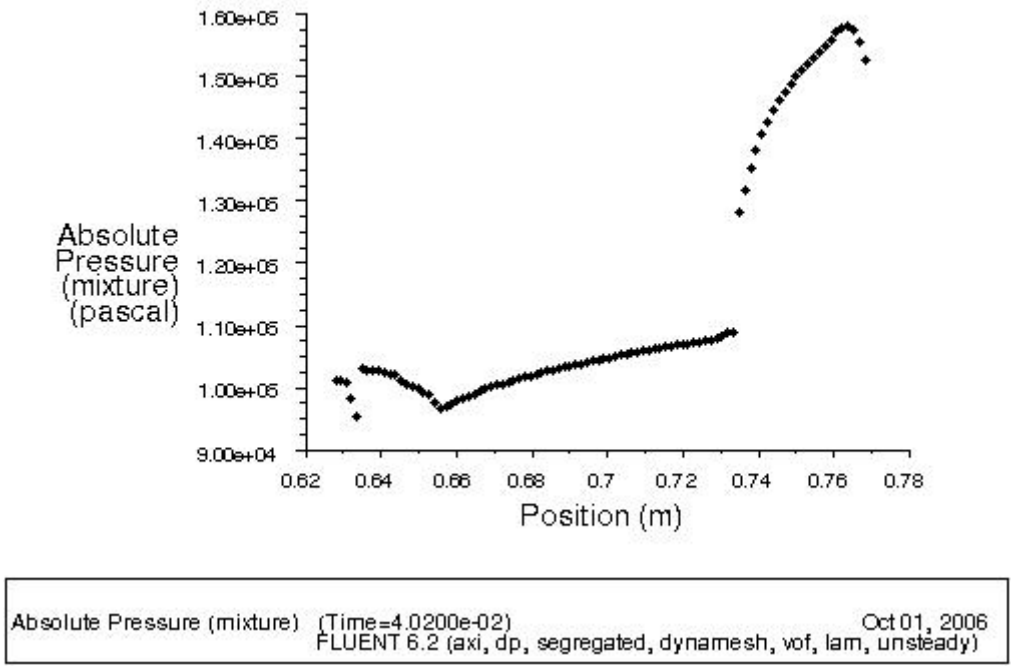

Figure 6: Pressure distribution along the penetrator for the second test

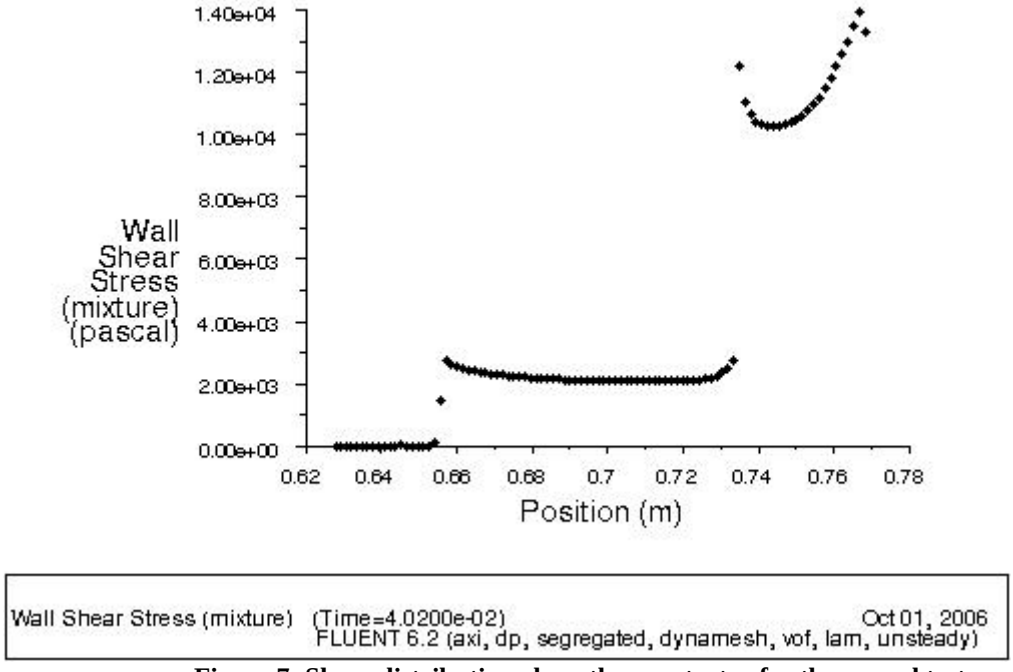

Figure 7: Shear distribution along the penetrator for the second test

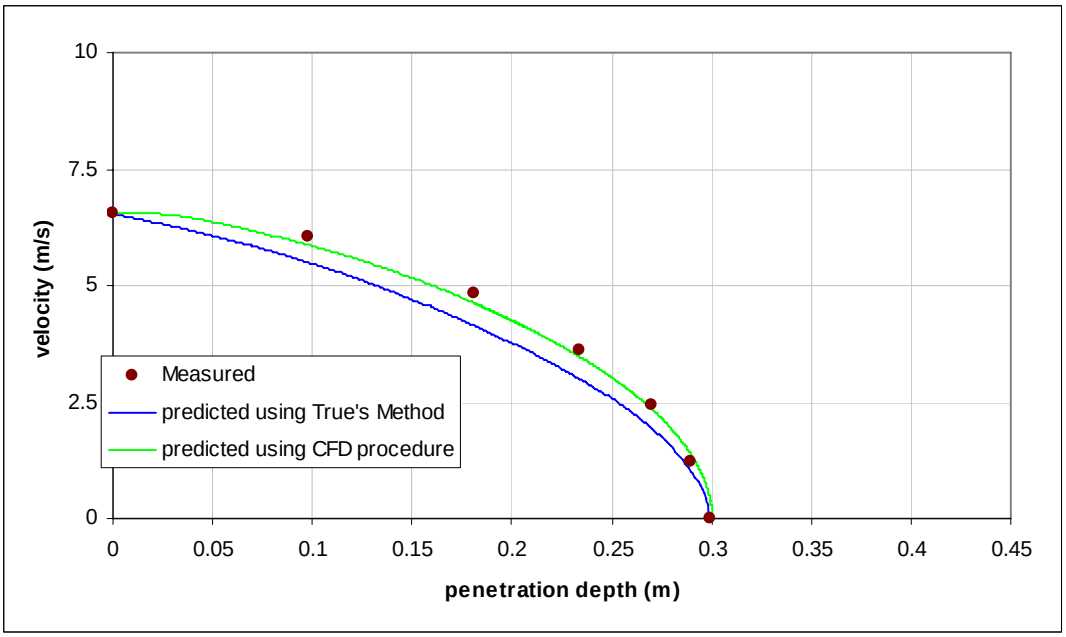

Figure 8: Measured velocity profile versus predicted profiles for the first test

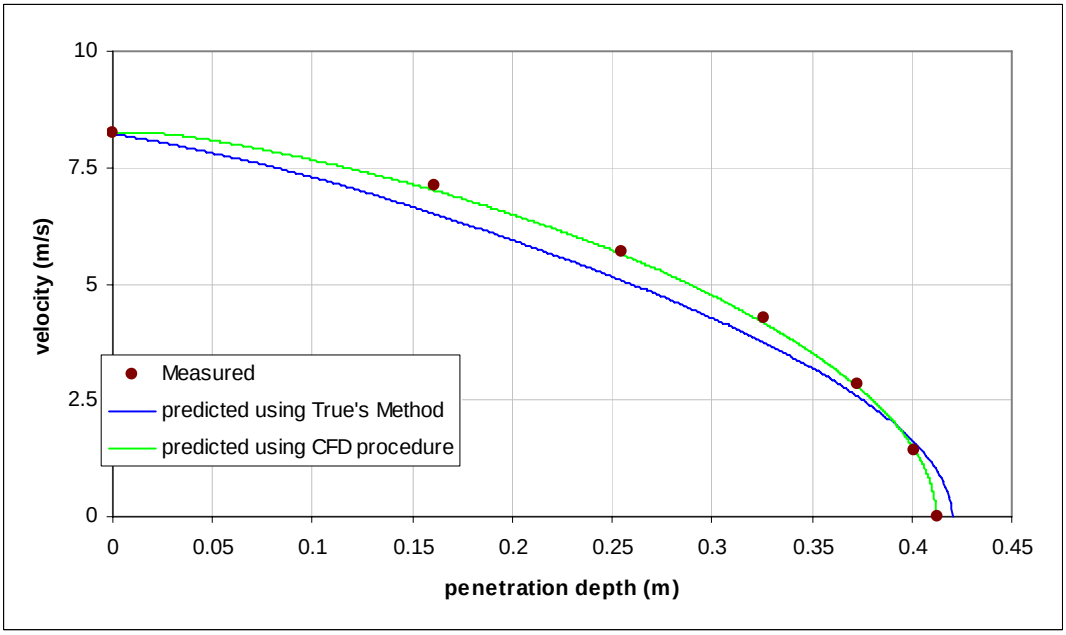

Figure 9: Measured velocity profile versus predicted profiles for the second test

Conclusion

A computational procedure based on computational fluid dynamics modeling was developed for the prediction of the embedment depth of torpedo anchors. The procedure not only is capable of estimating the embedment depth but provides the distribution of pressure and shear along the detailed geometry of penetrator. The CFD model was used in simulations of vertical penetration with pointed, axisymmetric penetrators. Results are promising with regard to embedment-depth estimation and, furthermore, the CFD

procedure provides estimates of the pressure and shear distributions on the soil-anchor interface. These distributions are of key significance in subsequent computations: soil reconsolidation in the vicinity of the anchor for the purpose of set-up studies, followed by pull-out capacity estimation.

Acknowledgment

This research was made possible with support from the Minerals Management Service and the Offshore Technology Research Center.

References

Araujo, J. B., Machado, R. D., Medeiros Jr., C. J. (2004). "High Holding Power Torpedo Pile - Results for the First Long Term Application." Proceedings of the 23rd International Conference on Offshore Mechanics and Arctic Engineering, Vancouver, British Columbia, Canada, pp 417-421.

Atturio, J. M., Valent, P. J. (1977). "High-Capacity, Deep-Water, Free-Fall Anchor." OCEANS, Volume 9, pp 592 – 596.

Audibert, J. M. E., Movant, M. N., Won, J., Gilbert, R. B. (2006). "Torpedo Piles: Laboratory and Field Research." Proceedings of the Sixteenth International Offshore and Polar Engineering Conference, San Francisco, California.

Ayabe, C., Costa, M. N. V., Leitao, H. L. F., Oliveria, N. V., Silva, S. H. S. C., Ribeiro, E. J. B. (2001). "Semi-Submersible Drilling Rig Petrobras X: Past and Future." Proceedings of the 20th International Conference on Offshore Mechanics and Arctic Engineering, Rio de Janeiro, Brazil.

Beard, R. M. (1984)." Expendable Doppler Penetrometer for Deep Ocean Sediment Strength Measurements." Naval Civil Engineering Laboratory, Report number: TR-905, Port Hueneme, California.

Brandao, F. E. N., Henriques, C. C. D., Araujo, J. B., Ferreira, O. C. G., Amaral, C. D. S. (2006). "Albacora Leste Field Development – FPSO P-50 Mooring System Concept and Installation." Proceedings of the 38th annual Offshore Technology Conference, Houston, Texas, Paper No. OTC 18243.

Ehlers, C. J., Young, A. G., Chen, J. (2004). "Technology Assessment of Deepwater Anchors." Proceedings of the 36th Annual Offshore Technology Conference, Houston, Texas, Paper No. OTC 16840.

FLUENT User's Guide (2006), Fluent Inc.

Freeman, T. J., Murray, C. N., Francis, T. J. G., McPhail, S. D., Schultheiss, P. J. (1984). "Modeling Radioactive Waste Disposal by Penetrator Experiments in the Abyssal Atlantic Ocean." Nature, Vol. 310, pp 130-133.

Freeman, T. J., Burdett, J. R. F., (1986). "Deep Ocean Model Penetrator Experiments." Final Report to Commission of the European Communities, Contract No. 392-83-7-WAS-UK.

Hickerson, J., Freeman, T. J., Boisson, J., Gera, F., Murray, N., Nakamura H., Nieuwenhuis, J. D., Schuller, K. H. (1988). "Feasibility of Disposal of High-level Radioactive Waste into the Seabed." Volume 4: Enginerring, Nuclear Energy Agency, Paris.

Lieng, J. T., Hove, F., Tjelta, T. I. (1999). "Deep Penetrating Anchor: Subseabed Deepwater Anchor Concept for Floaters and Other Installations." Proceedings of the 9th International Offshore and Polar Engineering Conference, Brest, France, pp 613-619.

Lieng, J. T., Kavli, A., Hove, F., Tjelta, T. I. (2000). "Deep Penetrating Anchor: Further Development, Optimization and Capacity Verification." Proceedings of the 10th International Offshore and Polar Engineering Conference, Seattle, Washington, pp 410-416.

Medeiros Jr., C. J. (2002). "Low Cost Anchor System for Flexible Risers in Deep Waters." Proceedings of the 34th Annual Offshore Technology Conference, Houston, Texas, Paper No. OTC 14151.

Medeiros Jr., C. J., Hassui, L. H. Machado, R. D., (1997). "Pile for Anchoring Floating Structures and Process for Installing the Same." United States Patent Number 6,106,199.

O'Loughlin, C. D., Randolph, M. F., Richardson, M. (2004). "Experimental and Theoretical Studies of Deep Penetrating Anchors." Proceedings of the 36th annual Offshore Technology Conference, Houston, Texas, Paper No. OTC 16841.

True, D. G. (1975). "Penetration of Projectiles into Seafloor Soils." Naval Civil Engineering Laboratory, Report number: R-822, Port Hueneme, California.

True, D. G. (1976). "Undrained Vertical Penetration into Ocean Bottom Soils." PhD Dissertation, University of California, Berkeley, California.

Zimmerman E. H., Spikula, D. (2005). "A New Direction for Subsea Anchoring and Foundations." <http://www.sname.org/sections/texas/Meetings/Presentations>.